MODELING AND SIMULATION OF WELDLINES IN INJECTION MOLDING PROCESS

Khaled Mezghani[1]

1:King Fahd University of Petroleum and Mineral, box 169 Dhahran 3262 Saudi Arabia.

E-mail: mezghani@kfupm.edu.sa

ABSTRACT

During the last few decades, considerable developments have been achieved in the area of computer-aided polymer processing, such as: injection molding, thermoforming, and profile extrusion. Injection molding is one of the most important processes of thermoplastic materials. Even though injection molding is simple in principle the real process is quite complex. The complexity of the problem rises from the unsteady and non-isothermal process and the rheological behavior of the molten polymer. The problem is generally solved using numerical techniques and realistic rheological models for quantitative analysis. Usually a good process simulation will predict the final shape of the product and the location of different defects. One of the major defects in the injection molding process is the formation of weldlines that lead to surface imperfections and weak spots in the part. A weldline is a three dimensional region with complex morphology. The location of the weldline is highly dependable on the location of the gates in the mold and the shape of the product. In this paper two different parts with visible weldlines will be compared to the simulation results. The prediction of the weldline location in a relatively complex shape is in good agreement with the real product.

Keywords: *injection, molding, weldline, orientation, viscosity, polymer, defect, process.*

الملخص

في خلال العقود الأخيرة القليلة وصل العالم الى تقدم هائل في ميدان برمجة الحاسب الألي (الحاسوب) لمساعدة تصنيع اللدائن (البلاستيك) مثل برامج التشكيل بالحقن (الحقن في القوالب). رغم أن عملية التشكيل بالحقن سهلة في المبدأ الا أنها معقدة من حيث التصنيع. هذا التعقيد في الصناعة ناتج عن عدم استقرار العملية الصناعية المتعاقبة و عدم موازنة الحرارة و كذلك سيولة المواد البلاستيكية التي عادة ما تكون معقدة, حيث أنها تعتمد على الحرارة و الظغط وسرعة الأنبثاق. لذلك أستخدمت بعض برامج الحاسوب لتوقع شكل القطع المصنعة بكل دقة وتفاصيل التي تبين للصانع نقط الضعف و الخلل في القطع المصنعة. من هذه العيوب الظاهرة خط اللحام, وهو عبارة عن تلاقي مقدمة السوائل القادمة من الاتجاه المعاكس. في هذا البحث استعمل برنامج "س-مولد" لتقدير مواقع خط اللحام في بعض القطع البلاستيكية.

1. INTRODUCTION

Injection molding process involves the rapid pressure filling of a specific mold cavity with a fluid material, followed by the solidification of the material into a product. After sufficient time for the plastic part to solidify (usually by cooling), the mold opens and the part is removed. The injection molding process is used for thermoplastics, thermosetting resins, and rubbers.

Injection molding makes discrete parts that can have complex and variable cross-sections as well as a wide variety of surface textures and characteristics. The wide variety in the types of parts that can be made by injection molding is a key reason that more injection molding machines are used for plastics processing than any other type of molding equipment. Another important reason for the popularity of injection molding is that parts are highly repeatable, that is, the parts can be made with very little part-to part variation.

Even though injection molding is simple in principle the real process is quite complex. The complexity of the problem give rise to many defects such as molecular orientation, warpage, shrinkage, sink lines, weldlines, etc… .In this paper we will mainly discuss the weldline location and prediction.

A weldline (also called a weld mark or a knit line) is formed when separate melt fronts traveling in opposite directions meet. A weldline is a three dimensional region with complex morphology. The location of the weldline is highly dependable on the location of the gates in the mold and the shape of the product. Weldlines are generally undesirable when part strength and surface appearance are major concerns. This is especially true with fiber-reinforced materials, because the fibers do not bridge the weldlines and often are oriented parallel to them, as illustrated in Figure 1 below. Likewise, the molecular orientation of an injected polymer is expected to follow the representation of Figure 1. The exact strength of the weldline depends on the ability of the flow fronts to weld (or knit) to each other. The strength of the weldline area can be from 10 to 90 percent as strong as the pure material used. Usually, a good design would locate the weldline in areas with the lowest stress; therefore, the prediction of the weldline location is very important for a successful product. For a product with simple geometry the prediction of the weldline is relatively easy; however, a complex geometry requires good simulation package software. Among several software packages, C-Mold has good reputation in simulating the polymer flow during injection molding process and predicting possible defects in the product.

C-MOLD is a set of integrated computer aided engineering (CAE) simulations for plastics molding processes, including injection molding filling, post-filling, cooling, and part shrinkage and warpage. C-MOLD provides solutions in all stages of design and manufacturing to improve productivity and enhance part quality. For complex part geometry, flow simulation helps to predict the weldline position with respect to changes in the tool design, and to monitor the temperature difference.

The complexity of both the process (non-isothermal, unsteady) and the rheological behavior of the molten material generally require the use of numerical techniques and realistic rheological models for quantitative analysis. Literature reviews on the numerical simulation of injection molding can be found in Hieber and Shen [Hieber ;Shen, 1980],

Top

Chiang et al. [Chiang et al., 1991], Dupret and Vanderschuren [Dupret; Vanderschuren, 1988], Tucker [Tucker, 1989], Crochet et al. [Crochet et al. 1994], Dupret et al. [Dupret et al., 1999], and among others [Hofer; Fritz, 2001], [Ilinca, and Hetu, 2001], [Jansen, 1998], [Chiang et al. 1993], [Yokoyama; Yamane, 2001] and [Bingfeng et al., 2001].

The main concern of this paper is to predict the location of the weldline of two different products: one is a straight coupling, and the other is a T-coupling. Both products were made with chlorinated polyvinyl chloride (CPVC) and produced using injection molding process.

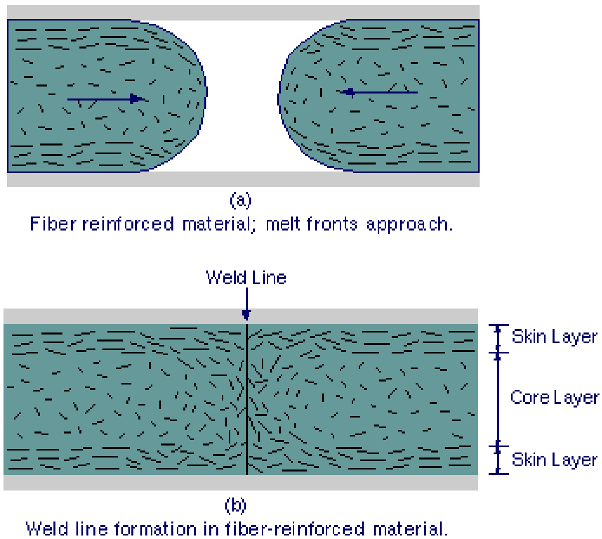

Figure 1: Fiber distribution parallel to the weldline leads to a weaker bond.

2. RESULTS AND DISCUSSION

In injection molding, three important variables have to be determined at each location inside the mold cavity. These variables consist of temperature, pressure, and velocity of the melt. The first two variables are controlled with the injection-molding machine; however, the velocity of the melt depends on the viscosity of the polymer, which in turn depends on temperature, pressure, and shear rate. Therefore, a complete mold filling simulation would require the calculation of the detailed velocity, pressure, and temperature profiles throughout the mold flow region, including the position and shape of the advancing front. This would suffice in principle to determine orientation distribution affecting the article morphology, which evolves upon cooling and solidification. Such a complete mode would be instrumental in assisting the theoretical mold design as well as in optimizing molding conditions for specified property requirements. The Complete problem, of course, is extremely complex even for a relatively simple mold. The complexity arises form the viscosity dependence on temperature, pressure, and shear rate. In addition, the temperature profile has to be determined at each point in the mold's cavity.

Top

The typical heat path in the cooling stage of injection molding consists of heat conducted from the hot polymer to the comparatively cold mold, then conducted through the mold to the cooling line, where it is convected away by the coolant. The cooling stage of the injection molding cycle is not ideal for a variety of reasons impacting both the product quality and production economics. As shown in Figure 2, the cold mold temperature conducts heat from the hot polymer melt causing the development of a skin on the exterior of the part and a propagation of frozen layers towards the core of the part. These frozen layers increase the flow resistance, making the mold cavity difficult to fill. Since frozen layers are developed continuously during injection and cooling, they "lock in" varying levels of stress and orientation. This variation in polymer morphology as a function of thickness and location reduces optical, structural, and other part properties. In addition, these frozen layers further complicate the problem of determining the temperature profiles as well as the melt flow velocity.

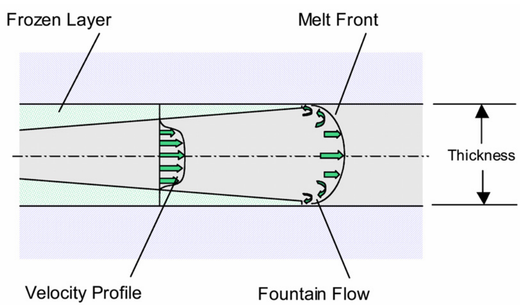

Figure 2: Schematic of polymer flow orientation during mold fill.

The melt flow velocity requires a good understanding of the melt rheology, which is the most important property used in flow simulations. Most polymers exhibit two regimes of flow behavior, Newtonian and shear thinning. Newtonian flow occurs at low shear rates, but with increasing shear, the viscosity tends to fall away in what is termed shear-thinning behavior. For Newtonian fluids, such as water, viscosity is independent of the shear rate. However, for non-Newtonian fluids, which include most polymer melts, the viscosity varies, not only with temperature, but also with the shear rate. The typical shear rate, which is experienced by the polymer melt during the injection molding process, ranges from 10^2 to 10^5 second^{-1}.

When the polymer is deformed, there will be some molecular disentanglement, slippage of chains over each other, and molecular alignment in the direction of the applied stress. As a result, the resistance exhibited by polymer to flow decreases with the deformation, due to the evolution of its microstructure (which tends to align in the flow direction). This is often referred to as shear-thinning behavior, which translates to lower viscosity with a high shear rate. Shear-thinning behavior provides some benefits for processing the polymer melt. For example, if the applied pressure to move water in an open-ended pipe is doubled, the flow rate of the water also doubles. However, in a similar situation using a polymer melt, if the pressure is doubled, the melt flow rate may increase from 2 to 15 times, depending on the material characteristics.

Top

Polymer viscosity also decreases with increasing temperature. Since the mobility of polymer molecular chains decreases with decreasing temperature, the flow resistance of polymer melt also greatly depends on the temperature. As shown in Figure 3, the melt viscosity decreases with increasing shear rate and temperature due to the disentanglement and alignment of the molecules and enhanced mobility of polymer molecules, respectively. In addition, the melt viscosity also depends on the pressure. The higher the pressure, the more viscous the melt becomes.

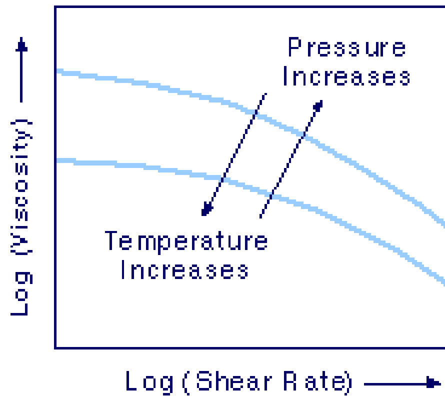

Figure 3: The viscosity of polymer melt depends on the shear rate, pressure, and temperature.

To incorporate the dependence of melt viscosity on shear rate ($\dot{\gamma}$), temperature (T), and pressure (p), the following 5-constant (n, τ^*, B, T_b, β) model is being used by C-Mold software for simulating the filling stage in injection molding.

$$\eta(T,\dot{\gamma},p)=\frac{\eta_o(T,p)}{1+\left(\frac{\eta_o\,\dot{\gamma}}{\tau^*}\right)^{1-n}}$$

with

$$\eta_o(T,p)=B\exp\left(\frac{T_b}{T}\right)\exp(\beta\, p)$$

This model handles both the Newtonian and the shear-thinning flow regions found in polymer rheology. The transition between the two regimes is characterized by τ^*, the shear stress at which shear thinning behavior begins to manifest itself. The slope of the shear-thinning curve is characterized by (1-n). The remaining three constants (B, T_b, β) are used to model the zero-shear-rate viscosity. For most polymer melts, rheology data spans both of these regions. However, in few cases the generation of a complete curve may not be possible. For example, if there are insufficient points in the shear-thinning region, the value of n might be erroneous. Similarly, if the data set lies almost entirely in the power-law region, the values of the zero-shear viscosity, η_o and τ^*, will tend to be ill-defined.

The use of the 5-constant model has generated successful results for this study. The analysis consists of two different types of specimen, which have apparent weldlines at their surfaces. These weldlines are present as knit lines of 0.3 mm width, at the inner and outer surfaces of each specimen. A four-inch-diameter straight coupling made of chlorinated polyvinyl chloride was bought from the local market. The drawing of the specimen is presented in Figure 4a. In C-Mold the thickness of the specimen is presented as a thin line; however, it is being considered in the simulation process. Following the drawing of the straight coupling, a finite-element mesh is generated. The injection point is selected at the same position as the actual specimen (Figure 4b). In the injection molding process, the gate location in the mold cavity is one of the key design parameters in the mold design. In fact, the gate location greatly affects the flow in the mold cavity by modifying the temperature distribution, the pressure, the weldline position, the fill time and the warpage after solidification. Using C-Mold simulation program and the actual location of the injection point, the melt front advancement is generated and presented in Figure 5a with 95% total filling. Also, the weldline location was accurately predicted as shown in Figure 5b. This prediction is exactly as presented in the form of a knit line in the actual specimen. In addition to the weldline prediction, the C-Mold software is able to predict the molecular orientation at the skin (Figure 6a) as well as at the core of the specimen (Figure 6b). This difference in molecular orientation is one of the major reasons for the weakness of the weldline.

The other specimen of the study is a four-inch-diameter T-coupling, which is presented in Figure 7a. The finite element mesh generation of the T-coupling and the injection point are shown in Figure 7b. Figure 8a represents the melt front advancement of the T-coupling. Once the advanced melt fronts meet, the weldline of the T-coupling is generated (Figure 8b). This prediction is very close to the actual weldline, which is observed as a knit line at the surface of the actual specimen. The only difference between the prediction and the actual position of the weldline is the upper tip of the weldline. In the actual specimen there are two separate weldlines at the upper side of the T-coupling. However, these two separate weldlines are very close to each other. The actual distance separating them is 7 mm. It is believed that this discrepancy between the predicted location of the weldline and the actual position is due to the limited number of the generated meshes. In addition, it was assumed in the simulation that the temperature profile of the mold is uniform. This may not be the case if a non-uniform cooling system is being used in the production line. The analysis, also, involves the simulation of the molecular orientations at the skin level as well as the core of the T-coupling, which are presented in figures 9a and 9b, respectively.

3. CONCLUSION

According to this study it was shown that the weldlines of two different specimens with different degree of complexity could be predicted using the C-Mold simulation analysis. The predictions of the weldline locations are close to the actual position of the weldline in the actual specimen, which is made from chlorinated polyvinyl chloride. In addition, the molecular orientation at the skin and the core of the specimens can be visualized. With these incites the mechanical properties as well as the weak point of the injected part can be predicted, which will help designer to optimize their designed product.

Top

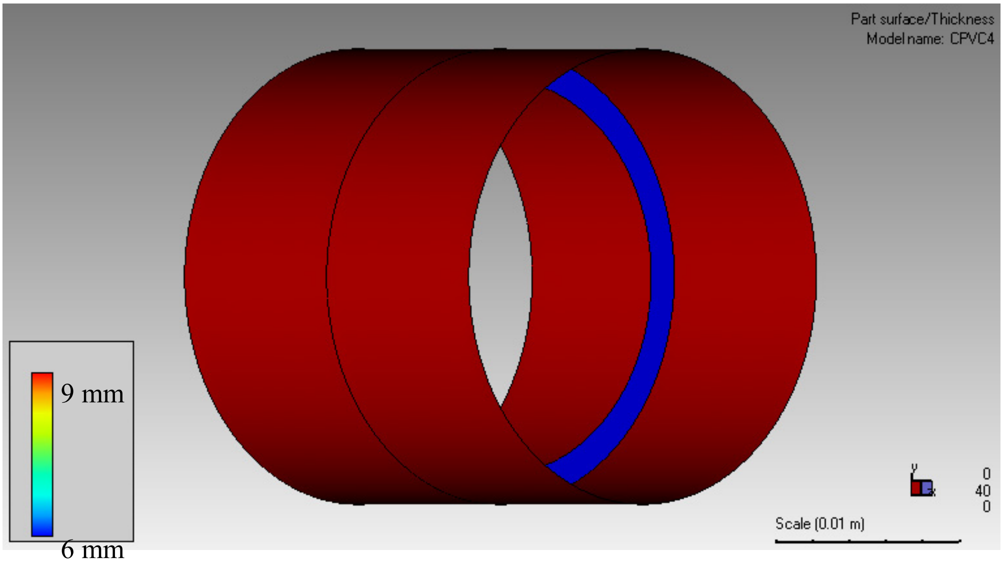

Figure 4a: Thickness distribution in the straight coupling. The wall (red) and the ring (blue) thickness are 9 and 6 mm, respectively.

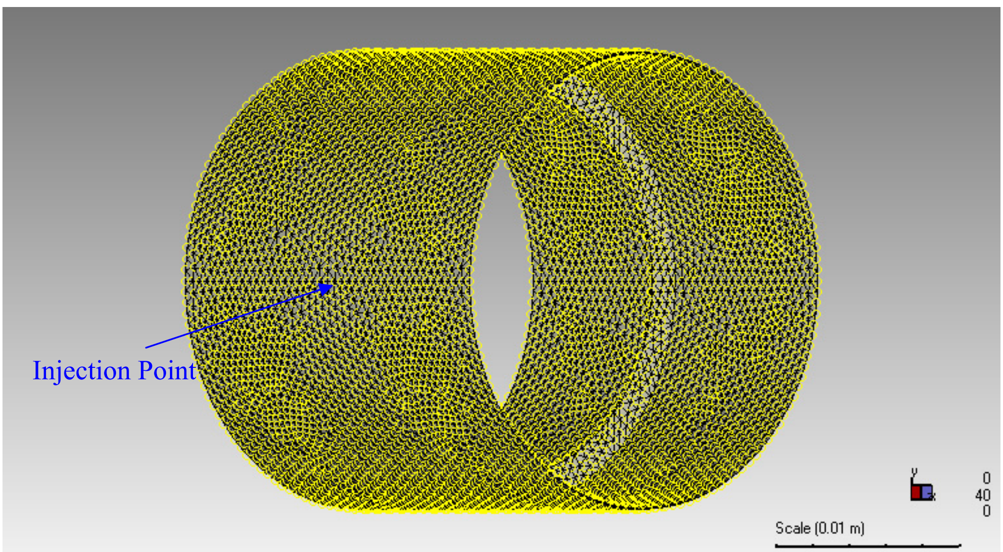

Figure 4b: Finite-element mesh of the straight coupling.

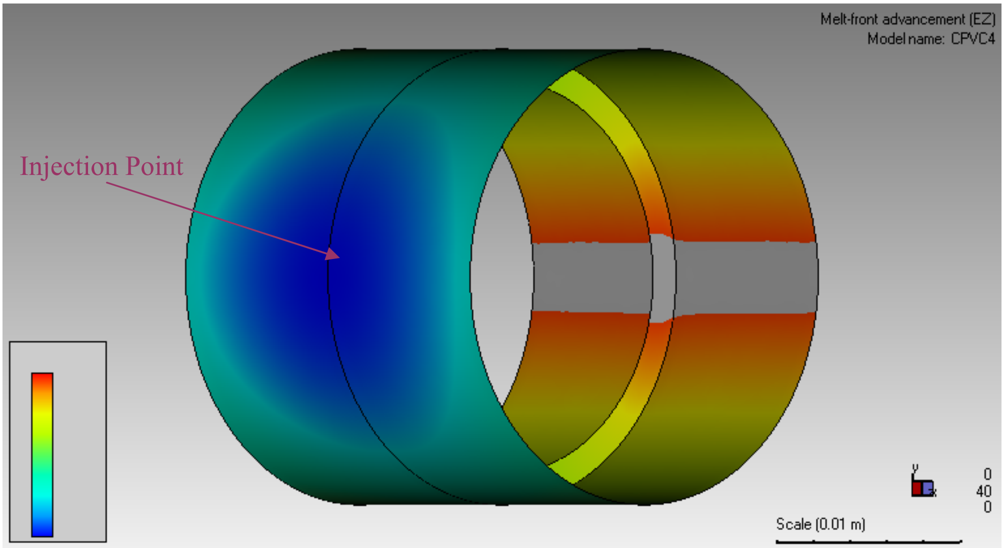

Figure 5a: Melt-front advancement in the straight coupling. This graph represents a 95% filling.

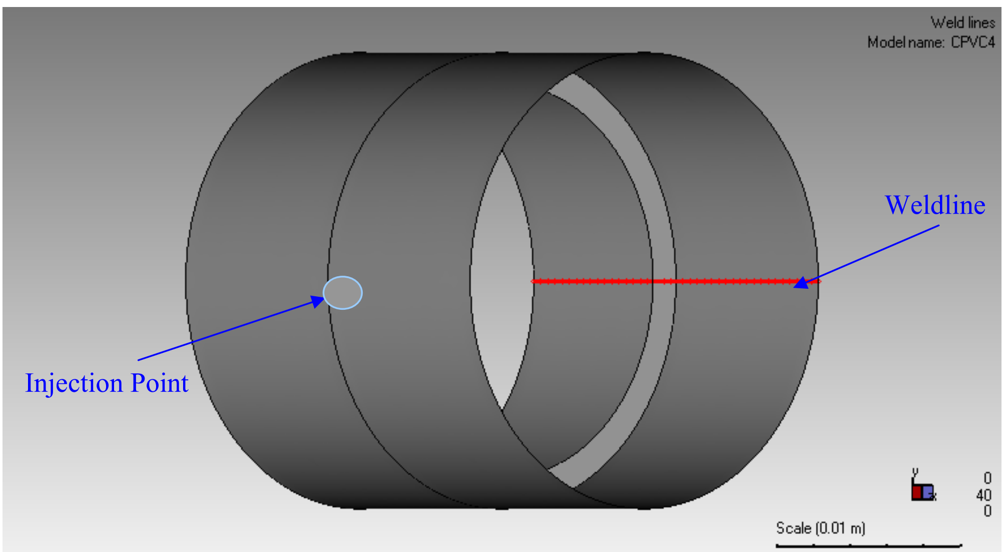

Figure 5b: Weldline prediction of the straight coupling.

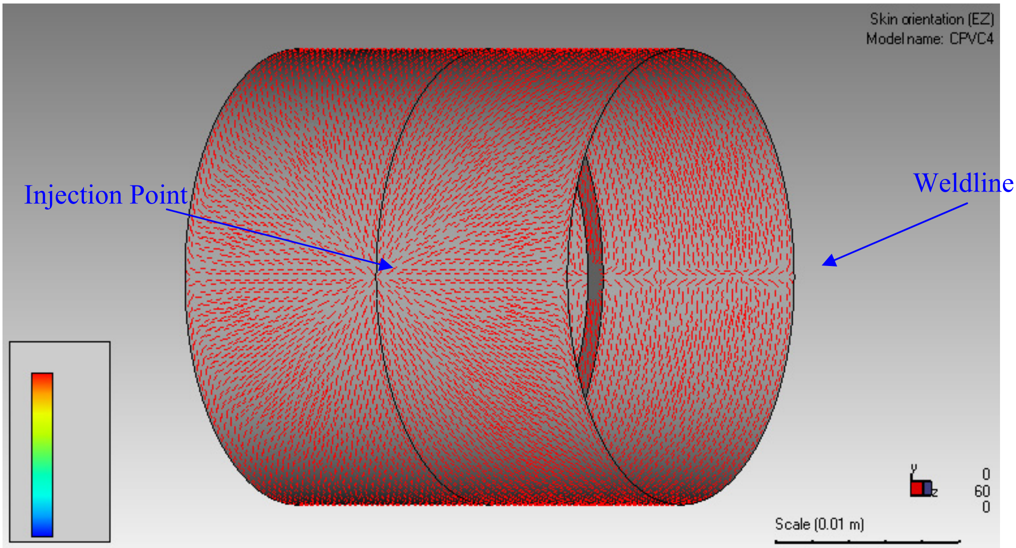

Figure 6a: Molecular orientation at the skin of the straight coupling.

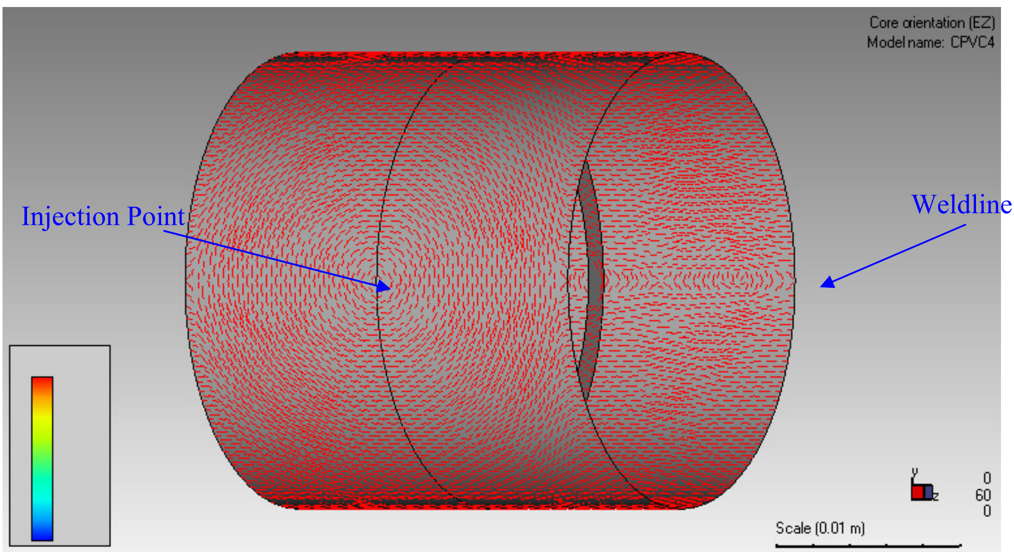

Figure 6b: Molecular orientation at the core of the straight coupling.

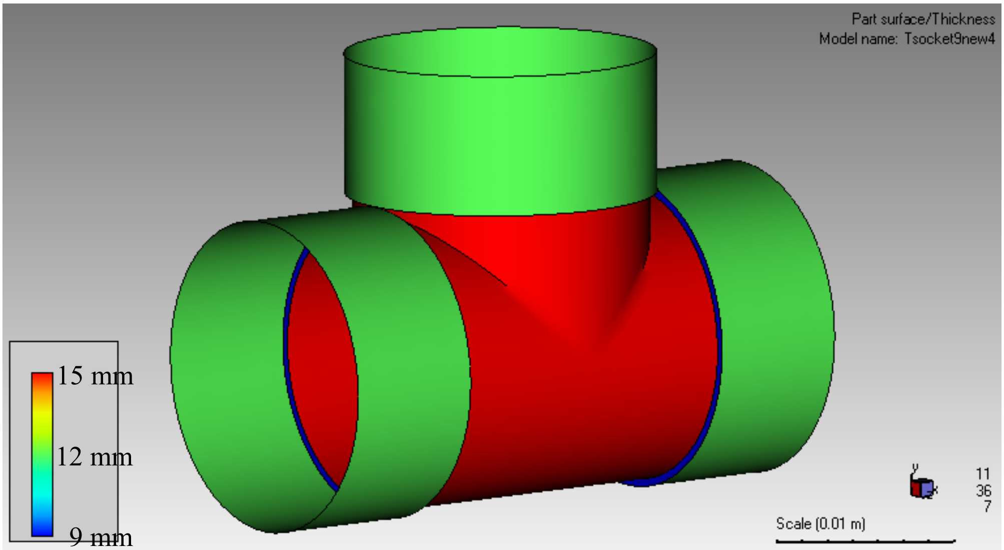

Figure 7a: Thickness distribution in the T-coupling.

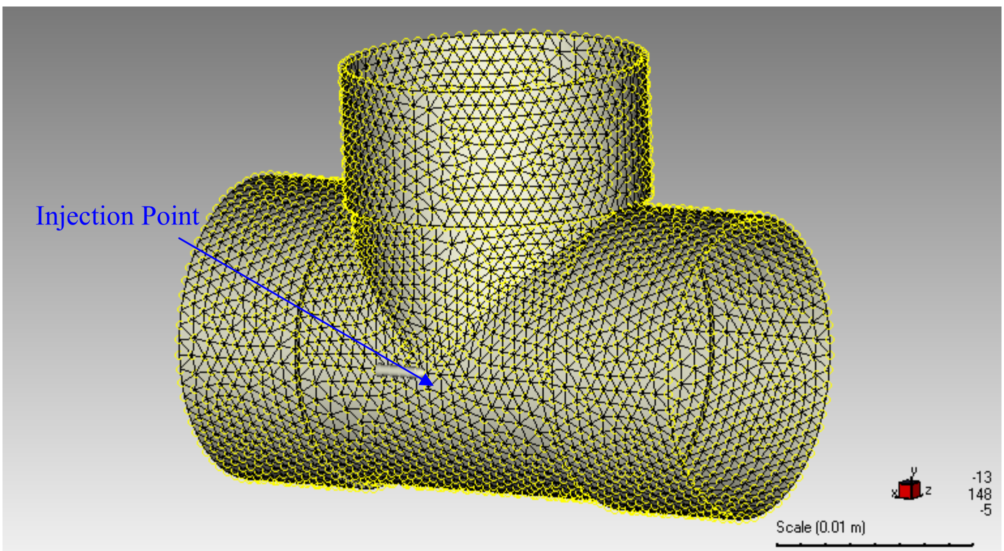

Figure 7b: Finite-element mesh of the T-coupling.

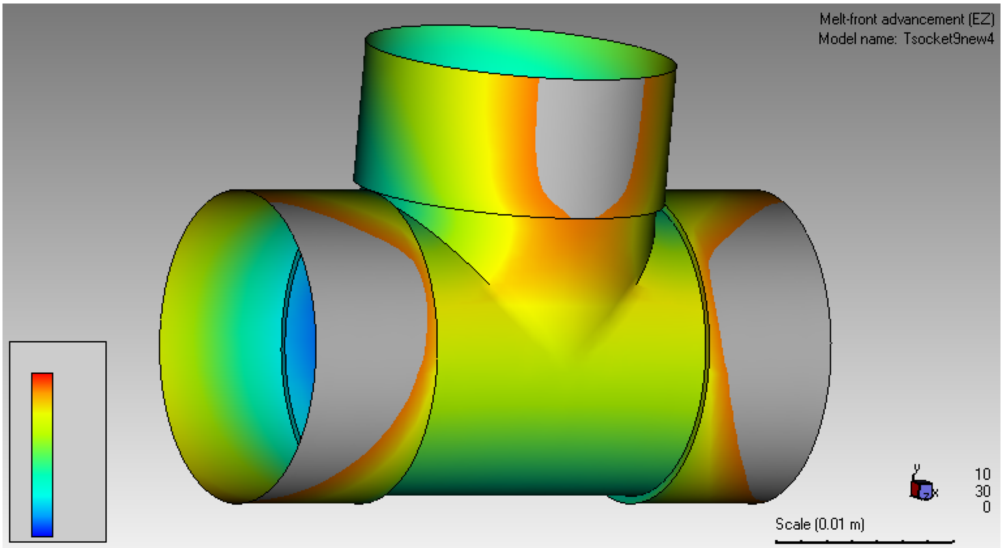

Figure 8a: Melt-front advancement in the T-coupling. This graph represents a total of 90% filling.

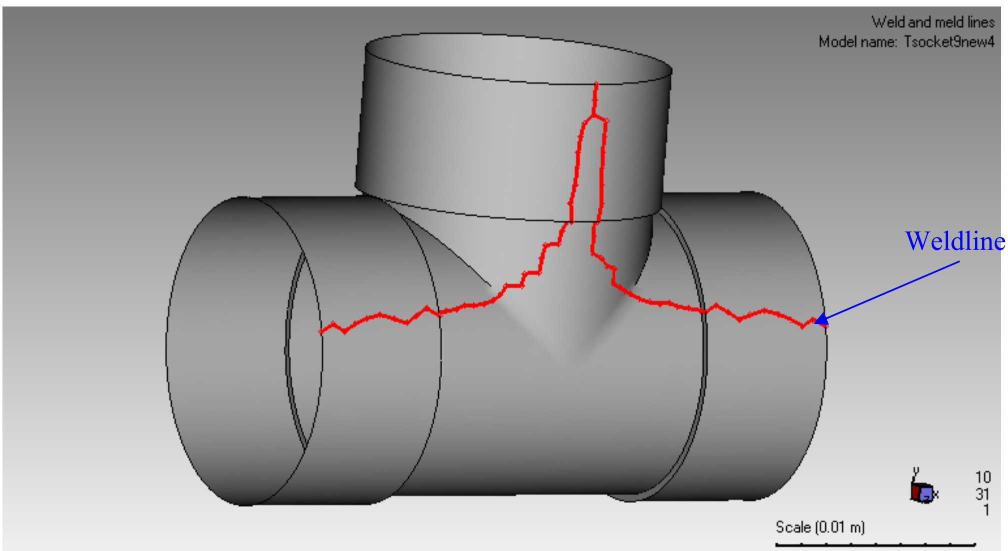

Figure 8b: Weldline prediction of the T-coupling.

Top

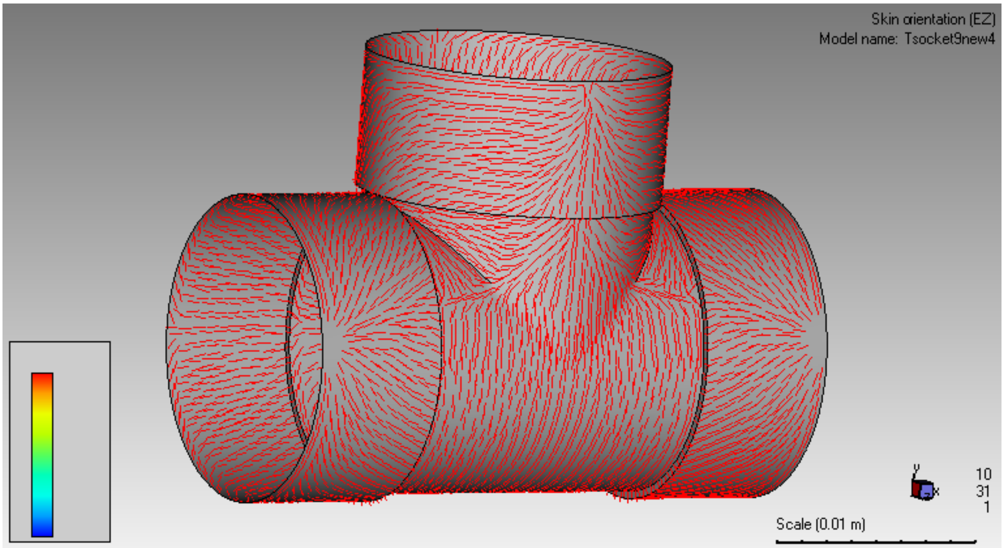

Figure 9a: Molecular orientation at the skin of the T-coupling.

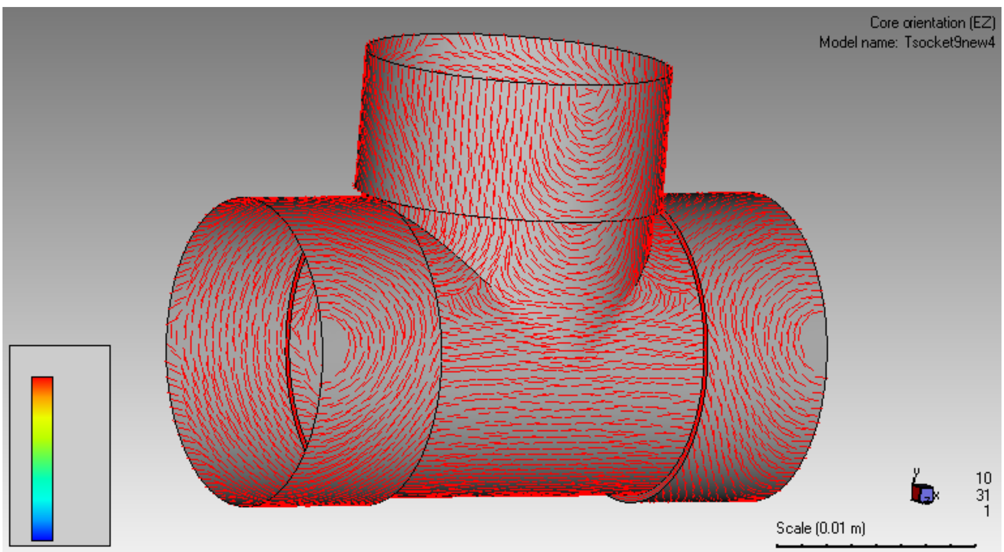

Figure 9b: Molecular orientation at the core of the T-coupling.

REFERENCES

1. Bingfeng, F.; Kazmer, D.; D. Hatch, 2001, "Simulation based optimization of injection molding", Polymer Processing Society Conf.
2. Chiang H.; Himasekhar, K.; Santhanam, N.; Wang. K., 193, "Integrated Simulation of Fluid Flow and Heat Transfer in Injection Molding for the Prediction of Shrinkage and Warpage," *Journal of Engineering Materials and Technology;* 115, pp. 37-47.
3. Chiang, H.H.; Hieber, C.A.; Wang, K.K., 1991, "A Unified Simulation of the Filling and Post-Filling Stages in the Injection-Molding, Part I: Formulation; Part II: Experimental Verification," *Polymer Engineering & Science,* 31 (2), pp. 116-139.
4. Crochet, M.J.; Dupret, F.; Verleye, V., 1994, "Injection Molding, In Flow and Rheology in Polymer Composites Manufacturing," pp. 415-463, edited by S.G. Advani, Elsevier.
5. Dupret, F.; Couniot, A.; Mal, O.; Vanderschuren, L.; Verhoyen, O., 1999, "Modeling and Simulation of Injection Molding: Advances in the Flow and Rheology of Non-Newtonian Fluids," D.A. Siginer, D. De Kee and R.P. Chhabra editors, Rheology Series, Elsevier, Amsterdam.
6. Dupret, F.; Vanderschuren, L., 1988, "Calculation of the temperature field in injection molding," AIChE Journal, 4 (12), pp. 1959-1972.
7. Hieber, C.A.; Shen, S.F., 1980, "A finite element/finite-difference simulation of the injection molding filling process," J. Non-Newt. Fl. Mech., 7, pp. 1-32.
8. Hofer, Th.; Fritz, H.G. 2001, "Modeling and Simulation of the Injection–Compression Molding Process for Thin-Wall Parts" Polymer Processing Society Conf.
9. Ilinca, F., and Hetu, J. F., 2001, "Three-Dimensional Filling and Post-Filling Simulation of Polymer Injection Molding," International Polymer Processing, 16 (3), pp. 291-301.
10. Jansen, K.M., 1998, "Measurements and Prediction of Anisotropy in Injection Moulding PP Products," International Polymer Processing, 13 (3), pp. 309-317.
11. Tucker III, C.L., 1989, "Computer Modeling for Polymer Processing," Hanser Publisher.
12. Yokoyama, A.; Yamane, S., 2001, "Optimum design technique for injection molding," Polymer Processing Society Conf.